

downhill currents is quite general and not restricted only to DLCs. However, it is important to note that the existence of downhill currents is a necessary but not sufficient condition for achieving ultrasmoothness. Amorphicity is another important prerequisite. Indeed, a transition to nanocrystallinity at higher temperatures or at higher impact energies is accompanied by considerable surface roughening also in the case of DLC films (8, 9, 17).

In summary, the multiscale theory presented here explains the origin of the ultrasmoothness of DLC coatings. Atomistic impact-induced downhill currents are responsible for the rapid erosion of asperities. Our detailed theoretical predictions are in excellent agreement with experiments. Our model is not restricted to ta-Cs. It can also be applied to explain the smoothness of other amorphous coatings deposited at high ion energy, the ion polishing of smooth surfaces, the chemical vapor deposition of hydrogenated tetrahedral amorphous carbon films, and the surface evolution of DLC films overgrown on structured substrates.

References and Notes

1. J. Robertson, *Mat. Sci. Eng. R* **37**, 129 (2002).
2. A. C. Ferrari, *Surf. Coat. Technol.* **180**, 190 (2004).
3. M. Allon-Aluf, J. Appelbaum, M. Maharizi, A. Seidman, N. Croitoru, *Thin Solid Films* **303**, 273 (1997).

4. J. Brand, G. Beckmann, B. Blug, G. Konrath, T. Hollstein, *Ind. Lubr. Tribol.* **54**, 291 (2002).
5. R. Hauert, *Diamond Relat. Mater.* **12**, 583 (2003).
6. J. P. Sullivan, T. A. Friedmann, K. Hjort, *MRS Bull.* **26**, 309 (2001).
7. A. C. Ferrari *et al.*, *Phys. Rev. B* **62**, 11089 (2000).
8. Y. Lifshitz, G. D. Lempert, E. Grossman, *Phys. Rev. Lett.* **72**, 2753 (1994).
9. X. Shi, L. Cheah, J. R. Shi, S. Zun, B. K. Tay, *J. Phys. C* **11**, 185 (1999).
10. C. Casiraghi *et al.*, *Phys. Rev. Lett.* **91**, 226104 (2003).
11. J. Robertson, *Thin Solid Films* **383**, 81 (2001).
12. P. R. Goglia, J. Berkowitz, J. Hoehn, A. Xidis, L. Stover, *Diamond Relat. Mater.* **10**, 271 (2001).
13. D. Li, M. U. Guruz, C. S. Bhatia, *Appl. Phys. Lett.* **81**, 81 (2002).
14. T. Yamamoto, Y. Kasamatsu, H. Hyodo, *Fujitsu Sci. Techn. J.* **37**, 201 (2001).
15. Y. Lifshitz, S. R. Kasi, J. W. Rabalais, *Phys. Rev. Lett.* **62**, 1290 (1989).
16. J. Schwan *et al.*, *J. Appl. Phys.* **79**, 1416 (1996).
17. Z. W. Zhao, B. K. Tay, L. Huang, G. Q. Yu, *J. Phys. D Appl. Phys.* **37**, 1701 (2004).
18. A. L. Barabasi, H. E. Stanley, Eds., *Fractal Concepts in Surface Growth* (Cambridge Univ. Press, Cambridge, 1995).
19. X. L. Peng, Z. H. Barber, T. W. Clyne, *Surf. Coat. Technol.* **138**, 23 (2001).
20. G. Pearce, N. Marks, D. McKenzie, M. Bilek, *Diamond Relat. Mater.* **14**, 921 (2005).
21. T. Frauenheim *et al.*, *J. Phys. Condens. Matter* **14**, 3015 (2002).
22. D. W. Brenner, *Phys. Rev. B* **42**, 8458 (1990).
23. H. U. Jäger, K. Albe, *J. Appl. Phys.* **88**, 1129 (2000).
24. M. Moseler, O. Rattunde, J. Nordiek, H. Haberland, *Nucl. Instrum. Methods B* **164-165**, 522 (2000).
25. O. Rattunde *et al.*, *J. Appl. Phys.* **90**, 3226 (2001).
26. The impact of a series of atoms with random impact

points $u = (u_1, u_2)$ on the surface $h = x_1 \tan \alpha$ results in an average transport of

$$\delta = \int d^2u \int_{-\infty}^0 dx_1 \int_0^{\infty} dx_1' t(x_1 - u_1, x_1' - u_1) - t(x_1' - u_1, x_1 - u_1) = \left\langle \sum_j d_1^{(j)} \right\rangle$$

atoms per impact across the x_2 axis. Here, $\langle \rangle$ indicates the average over many impacts and $t(x_1, x_1') = \sum_{i=1}^N \delta(x_1^{(i)} - x_1) \delta(x_1^{(i)} + d_1^{(i)} - x_1')$ measures the number of atoms displaced from x_1 to x_1' upon the impact of an atom onto the origin $u = 0$. The initial lateral coordinates of the atoms in the system are denoted by $x_1^{(i)}$.

27. C. A. Davis, G. A. J. Amaratunga, K. M. Knowles, *Phys. Rev. Lett.* **80**, 3280 (1998).
28. S. Uhlmann, Th. Frauenheim, Y. Lifshitz, *Phys. Rev. Lett.* **81**, 641 (1998).
29. S. F. Edwards, D. R. Wilkinson, *Proc. R. Soc. London A* **381**, 17 (1982).
30. W. W. Mullins, *J. Appl. Phys.* **30**, 77 (1959).
31. E. Spiller *et al.*, *Appl. Opt.* **42**, 4049 (2003).
32. J. Tersoff, *Phys. Rev. B* **39**, 5566 (1988).
33. We thank B. Huber and P. Koskinen for technical assistance, M. Mrovec for fruitful discussions, and D. P. Chu for providing AFM facilities at the Epson Research Laboratory, Cambridge. This research is supported by the Fraunhofer MAVO for Multiscale Materials Modelling (MMM) and by the FOSTOMA project of the Wirtschaftsministerium Baden-Württemberg. Simulations were performed on the CEMI cluster of the Fraunhofer institutes EMI, ISE, and IWM. Funding from European Union project FAMOUS is acknowledged. A.C.F. acknowledges funding from The Royal Society.

9 May 2005; accepted 21 July 2005
10.1126/science.1114577

The Effect of Diurnal Correction on Satellite-Derived Lower Tropospheric Temperature

Carl A. Mears and Frank J. Wentz

Satellite-based measurements of decadal-scale temperature change in the lower troposphere have indicated cooling relative to Earth's surface in the tropics. Such measurements need a diurnal correction to prevent drifts in the satellites' measurement time from causing spurious trends. We have derived a diurnal correction that, in the tropics, is of the opposite sign from that previously applied. When we use this correction in the calculation of lower tropospheric temperature from satellite microwave measurements, we find tropical warming consistent with that found at the surface and in our satellite-derived version of middle/upper tropospheric temperature.

Much of the surface warming of Earth observed over the past century is understood to be anthropogenic (1, 2). In the upper air, the situation is less clear because of the relative paucity of data and short period of observation (3). In situ temperature measurements made by radiosondes have limited spatial coverage, particularly over large portions of the oceans, and are subject to a host of complications, including changing instrument types, configurations, and observation prac-

tices (4). For the past two decades, microwave radiometers flown on a series of National Oceanic and Atmospheric Administration (NOAA) polar orbiting weather satellites have provided a complementary source of observations, which have been used to calculate temperature here. Nine microwave sounding unit (MSU) instruments have been flown, with high-quality data extending from late 1978 to mid-2004. The MSU data suffer from a number of calibration issues and time-varying biases that must be addressed if they are to be used for climate change studies. For MSU channel 2 (MSU2), the data and its asso-

ciated biases have been analyzed by a number of groups, yielding warming trends over the 1979–2004 period ranging from 0.04 to 0.17 K per decade (5–9). Unfortunately, interpretation of the raw MSU2 measurements is complicated by the fact that 10 to 15% of the signal in MSU2 arises from the stratosphere, which is cooling more rapidly than either the surface or the troposphere is warming, thus canceling much of the warming signal. Recently, Fu *et al.* have used weighted combinations of different MSU channels to remove the stratospheric influence from MSU2 (10–12). However, this method is a statistical inference that depends, in part, on the vertical coherence of stratospheric trends, rather than a direct measurement of the troposphere (13).

A more direct measurement of the lower troposphere can be obtained by using the MSU nadir-limb contrast to extrapolate the channel 2 brightness temperatures downward and remove nearly all of the stratospheric influence (5, 14, 15) [supporting online material (SOM) text and fig. S1]. As originally constructed by Christy *et al.*, this nadir-limb product (TLT, or temperature lower troposphere) showed cooling relative to the surface in many regions of Earth, particularly in the tropics. This finding is at odds with theoretical considerations and the predictions of climate models (16–18), both of which predict that any warming at the surface would

Remote Sensing Systems, 438 First Street, Suite 200, Santa Rosa, CA 94501, USA.

be amplified in the tropical troposphere. The surface/TLT disconnect is a problem only on decadal time scales; on shorter time scales, the ratio of the temporal variability in the Christy *et al.* TLT to the temporal variability of the surface temperature agrees well with expectations (19, 20).

We present results from a new TLT analysis that uses a different, model-based, method to remove spurious trends caused by the slow evolution of each satellite's local measurement time over the diurnal cycle in atmospheric temperature. Each satellite typically exhibits a slow change of the local equator-crossing time (LECT) (Fig. 1A) and a decay of orbital height over time due to drag by the upper atmosphere (21). The LECT is the time at which the satellite passes over the equator, moving in a northward or "ascending" direction. Changes in LECT indicate corresponding changes in local observation time for the entire orbit. If the temperature being measured changes with the time of day (e.g., the diurnal cycle of daytime heating and nighttime cooling), slow changes in observation time can cause spurious long-term trends, which must be removed from each satellite's data record before attempting to merge the data together into a single data set (22).

Christy *et al.* estimated the effect of the diurnal cycle by calculating the mean rate of diurnal warming and cooling by subtracting the temperature measurements on one side of the satellite measurement swath from the other (15). This provided an estimate of the temperature change due to the difference in local observation times from one side of the satellite swath to another, about 40 min at the equator (23). Unfortunately, this method is extremely sensitive to small changes in the satellite attitude, particularly the satellite roll angle, calling its accuracy into question (SOM text).

In our work on MSU2, we used a different approach to evaluate the diurnal cycle. We used 5 years of hourly output from a climate model as input to a microwave radiative transfer model to estimate the seasonally varying diurnal cycle in measured temperature for each satellite view angle at each point on the globe (7). For the middle/upper troposphere (MSU2) on a global scale, there are no important differences between the two methods, although there are significant latitude-dependent differences (SOM text). In this work, we extend our method to TLT. In Fig. 1, B and C, we show a color-coded time-latitude plot of the corrections applied to TLT. For most latitudes, the Christy *et al.* TLT correction is of opposite sign from our TLT correction and from the corrections applied by either group for the middle/upper troposphere (fig. S2).

We argue that the sign change exhibited by the Christy *et al.* correction is physically

inconsistent with our understanding of the vertical structure of the diurnal cycle. For MSU2, the globally averaged diurnal cycle is dominated by the surface and near-surface diurnal cycle over land regions. This is supported by a number of findings: Maps of temperature differences between the ascending and descending MSU2 measurements show much larger differences over land than over ocean (7, 24). When these ascending/descending differences are examined as a function of Earth incidence angle, the differences are much larger for near-nadir angles than for larger incidence angles over land, suggesting that the bulk of the signal arises at or near the surface (fig. S3 and SOM

text), in general agreement with radiosonde measurements (25) and general circulation models, including the Community Climate Model 3 model we used to calculate our diurnal correction.

Surface and near-surface effects will be even more dominant for TLT, whose vertical weighting function peaks several kilometers closer to the surface and has a surface contribution roughly double that of MSU2. Thus, we expect the TLT diurnal cycle and diurnal correction to be similar in shape to the MSU2 diurnal cycle, but with larger amplitude. This is consistent with the diurnal correction we calculate from the climate model and is inconsistent with the Christy *et al.* correction.

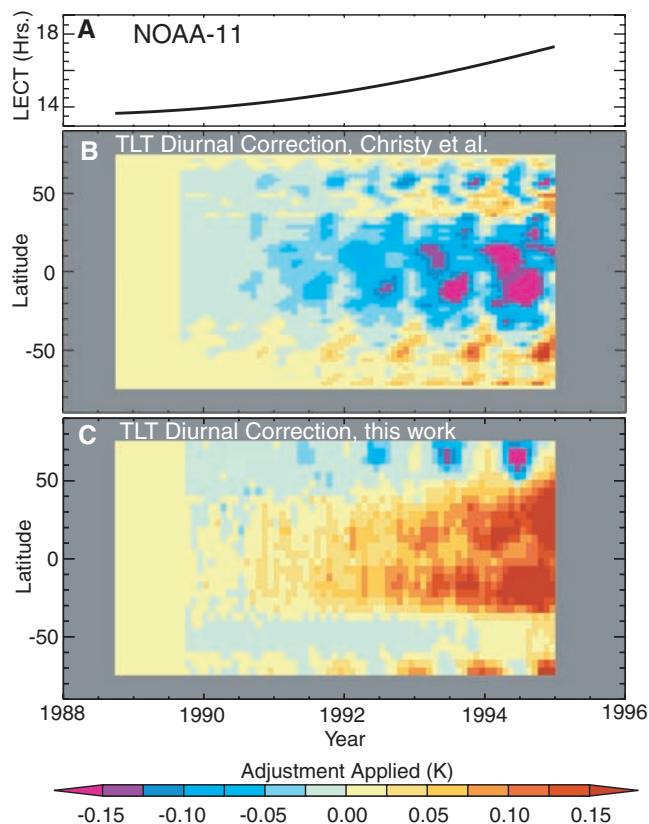


Fig. 1. Diurnal correction applied to MSU TLT for the NOAA-11 satellite. We use NOAA-11 as an example because it underwent a large drift in LECT of more than 6 hours before its ultimate failure in mid-1998. We show only the 1988–1993 period here because this is the only part of the NOAA-11 data used by Christy *et al.* NOAA-14 also underwent a similar drift, with its drift becoming more rapid after 1998, and by mid-2002, it had drifted by more than 4 hours. Most satellites in the MSU series drifted by at least 2 hours, with a few of the short-lived satellites drifting less than 1 hour. (A) LECT for the NOAA-11 satellite plotted as a function of time. (B) TLT correction applied by Christy *et al.* (C) TLT correction applied in this work.

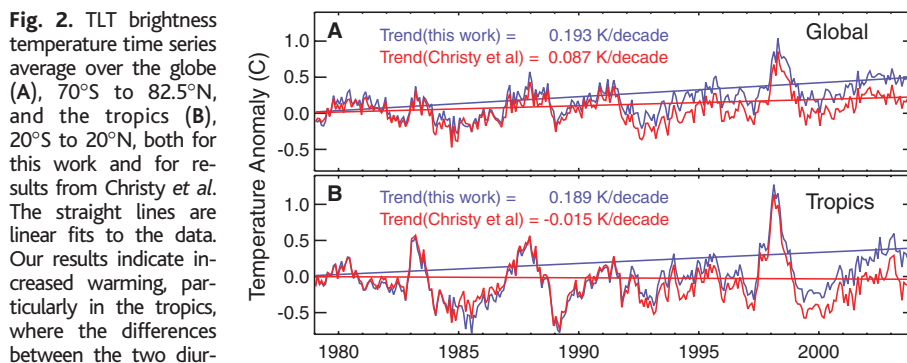


Fig. 2. TLT brightness temperature time series average over the globe (A), 70°S to 82.5°N, and the tropics (B), 20°S to 20°N, both for this work and for results from Christy *et al.* The straight lines are linear fits to the data. Our results indicate increased warming, particularly in the tropics, where the differences between the two diurnal corrections are the greatest. The differences between the time series become prominent after about 1991, when the drift in LECT for NOAA-11 begins to accelerate. A similar acceleration of drift in the NOAA-14 satellite occurs after 1998, with a corresponding increase in the difference between these time series.

The long-term behavior of a time series constructed from TLT is also dependent on the procedure used to merge the nine MSU satellites together into a single time series, in particular on the values of the parameters (“target factors”) used to empirically remove the spurious dependence of the instrument calibration on the temperature of the hot calibration target (5, 7, 15) (SOM text). For the results presented below, we used exactly the same merging procedure and target factors (but different offsets) as we used when producing our results for MSU2 (26).

When we merge the data from the nine MSU satellites together using both our diurnal correction and target factors, we obtain a long-term time series that shows substantially more warming than the Christy *et al.* result, particularly in the tropics. In Fig. 2, we show global and tropical average monthly anomaly time series for our analysis and for Christy *et al.* Our global (70°S to 82.5°N) trend of 0.193 K per decade (1979–2003) is about 0.1 K per decade warmer than the trend calculated over the same area from the Christy *et al.* data, whereas our trend in the tropics (20°S to 20°N) of 0.189 K per decade is about 0.2 K per decade warmer (27). We estimate the 2σ uncertainty in these trends to be 0.09 K per decade, including both internal and structural uncertainty (SOM text).

To estimate what portion of the trend difference between our respective results is caused by the difference in diurnal correction, we performed a set of numerical experiments, where we substituted the Christy *et al.* diurnal correction into our analysis, and/or where we fixed the values of the target factors to the values used by Christy *et al.*, allowing us to mimic different parts of the Christy *et al.* merging procedure separately and in combination. The results of these experiments (table S3) suggest that the difference in diurnal correction accounts for over 50% of the difference in trends for global averages and over 70% of the difference in trends for tropical averages.

In Fig. 3, we show global maps of TLT and surface trends (28) (1979–2003) and differences between these trends. The Christy *et al.* results indicate that the lower troposphere is cooling dramatically relative to the surface over almost all parts of the tropics, which is in sharp disagreement with both climate model output and theoretical arguments (20, 29). Our results suggest that the tropical troposphere is warming slightly more than the surface in most regions, in accordance with expectations, although scenarios where the tropical troposphere is cooling relative to the surface are also possible within the range of uncertainty.

Our results are also in agreement with middle tropospheric results obtained for our data by removing the stratospheric contamination in our MSU2 data using MSU channel 4 (10, 11), indicating a measure of vertical consistency in our results that is absent in the Christy *et al.* results (12). Also, the warming of the TLT in the tropics is in accordance with observed trends in total columnar water vapor from satellite observations made over the tropical oceans since 1988, which show an increase of more than 2% per decade (19, 30). Although the correlation of total water vapor and temperature is often limited to the boundary layer, it would be difficult to explain a moistening of the tropical atmosphere without some warming within the layer measured by TLT.

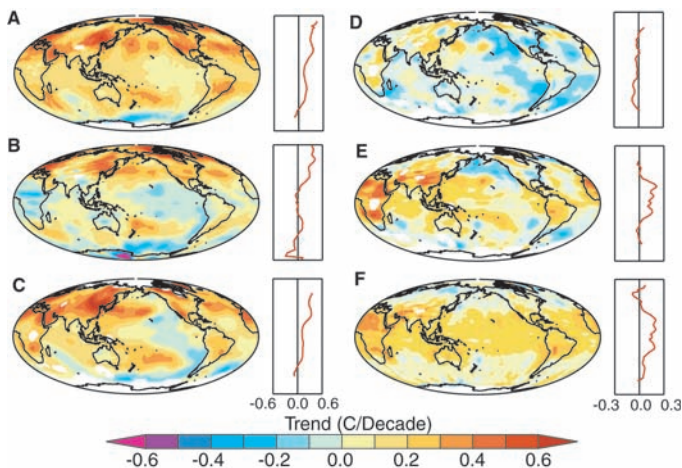
In contrast, trends from temporally homogenized radiosonde data sets show less warming than our results (31–33) and are in better agreement with the Christy *et al.* results. However, the radiosonde record is fraught with difficulties related to changes in instrument type, observing practices, data correction, and station location. In the tropics, where they are the largest, these problems have been shown to be more likely to lead to spurious cooling trends than spurious warming trends in the unadjusted data, suggesting the possibility that any problems that were not detected during homogenization may result in a cooling

bias in the homogenized radiosonde record (32). In the northern extratropics, there is excellent agreement between the Christy *et al.* results and a subsample of the radiosonde sites chosen to have consistent instrumentation type and thus thought to be relatively free of error (15). Presumably the agreement between these radiosondes and our data would be somewhat worse, although this has not been tested.

References and Notes

1. J. E. Hansen *et al.*, *J. Geophys. Res.* **106**, 23947 (2001).
2. J. T. Houghton *et al.*, *Climate Change 2001: The Scientific Basis: Contribution of Working Group I to the Third Assessment Report of the Intergovernmental Panel on Climate Change* (Cambridge Univ. Press, Cambridge, 2001).
3. J. W. Hurrell, S. J. Brown, K. E. Trenberth, J. R. Christy, *Bull. Am. Meteorol. Soc.* **81**, 2165 (2000).
4. D. J. Gaffen, M. A. Sargent, R. E. Habermann, J. R. Lanzante, *J. Clim.* **13**, 1776 (2000).
5. J. R. Christy, R. W. Spencer, W. B. Norris, W. D. Braswell, D. E. Parker, *J. Atmos. Ocean. Tech.* **20**, 613 (2003).
6. C. Prabhakara, J. R. Iacovazzi, J.-M. Yoo, G. Dalu, *Geophys. Res. Lett.* **27**, 3517 (2000).
7. C. A. Mears, M. C. Schabel, F. J. Wentz, *J. Clim.* **16**, 3650 (2003).
8. K. Y. Vinnikov, N. C. Grody, *Science* **302**, 269 (2003).
9. N. C. Grody, K. Y. Vinnikov, M. D. Goldberg, J. T. Sullivan, J. D. Tarpley, *J. Geophys. Res.* **109**, D24104 (2004).
10. Q. Fu, C. M. Johanson, S. G. Warren, D. J. Seidel, *Nature* **429**, 55 (2004).
11. Q. Fu, C. M. Johanson, *J. Clim.* **17**, 4636 (2004).
12. Q. Fu, C. M. Johanson, *Geophys. Res. Lett.* **32**, L10703 (2005).
13. S. Tett, P. Thorne, *Nature*, published online 2 December 2004 (10.1038/nature03208).
14. R. W. Spencer, J. R. Christy, *J. Clim.* **5**, 858 (1992).
15. J. R. Christy, R. W. Spencer, W. D. Braswell, *J. Atmos. Ocean. Tech.* **17**, 1153 (2000).
16. B. D. Santer *et al.*, *Science* **287**, 1227 (2000).
17. J. M. Wallace *et al.*, *Reconciling Observations of Global Temperature Change* (National Research Council, Washington, DC, 2000).
18. B. D. Santer *et al.*, *Science* **300**, 1280 (2003).
19. F. J. Wentz, M. Schabel, *Nature* **403**, 414 (2000).
20. B. D. Santer *et al.*, *Science* **309**, 1551 (2005); published online 11 August 2005 (10.1126/science.1114867).
21. The decay of orbital height also has an important effect on measurements of long-term temperature trends (34). This adjustment is done in the same way in the work reported here and in (15). Because it is not a cause of the current discrepancy, we do not discuss it further.
22. Both at Earth’s surface and in the troposphere, the diurnal cycle in temperature is dominated by the first harmonic. At a given point on Earth, the ascending and descending passes of the NOAA satellites make measurements separated by approximately 12 hours, so that averaging together the data from ascending and descending orbits has the effect of removing most of the first harmonic of the diurnal cycle. This cancellation becomes less effective as one moves toward the polar regions, where the local measurement times become closer together. We define diurnal correction to be the removal of any residual effects remaining after averaging the ascending and descending parts of the orbit together.
23. The cross-scan time difference grows slowly to about an hour at 45°N or S and to more than 2 hours in the polar regions.
24. C. A. Mears, M. Schabel, F. J. Wentz, B. D. Santer, B. Govindasamy, *Proc. Int. Geophys. Remote Sensing Symp. III*, 1839 (2002).
25. D. J. Seidel, M. Free, J. Wang, *J. Geophys. Res.* **110**, D09102 (2005).

Fig. 3. Global maps and zonal averages of linear temperature trends (1979–2003). Missing data are shown as white areas. (A) TLT temperature trends from this work. (B) TLT temperature trends from Christy *et al.* (5). (C) Surface temperature trends from (28). Trend difference, surface minus TLT, (D) this work and (E) Christy *et al.* (F) TLT trend difference, this work minus Christy *et al.*



26. We chose these values of the target factors to produce our final results because we have concluded that they are the most likely to be free of errors. They are calculated from oceanic observations to reduce errors from uncorrected diurnal variations, and we use unweighted MSU channel 2 data (T2 in SOM) to avoid additional noise due to the differencing procedure used to calculate TLT. The values of the intersatellite offsets needed to be recalculated to remove obvious intersatellite differences. In the supporting online material, we discuss the impact of using different data subsets to determine the target factors. This information is used to help determine the structural uncertainty.
27. We obtain this estimate of the tropical TLT trend when we recalculate the intersatellite offsets to optimize them for tropical data. If this reoptimization is not performed, as it is not in producing maps such as those shown in Fig. 3, we obtain a smaller trend value of 0.164 K per decade.
28. T. M. Smith, R. W. Reynolds, *J. Clim.* **18**, 2021 (2005).
29. J. W. Hurrell, K. E. Trenberth, *J. Clim.* **11**, 945 (1998).
30. K. E. Trenberth, J. Fasullo, L. Smith, *Clim. Dyn.*, in press; published online 11 May 2005 (10.1007/s00382-005-0017-4).
31. J. Lanzante, S. Klein, D. Seidel, *J. Clim.* **16**, 224 (2003).
32. J. Lanzante, S. Klein, D. Seidel, *J. Clim.* **16**, 241 (2003).
33. P. W. Thorne *et al.*, *J. Geophys. Res.*, in press.
34. F. J. Wentz, M. Schabel, *Nature* **394**, 661 (1998).
35. This work was supported by the NOAA Climate and

Global Change Program. We thank J. Christy and R. Spencer for providing numerical values for their diurnal adjustment.

Supporting Online Material
www.sciencemag.org/cgi/content/full/1114772/DC1
SOM Text
Figs. S1 to S4
Tables S1 to S3
References and Notes

12 May 2005; accepted 27 July 2005
Published online 11 August 2005;
10.1126/science.1114772

Include this information when citing this paper.

Amplification of Surface Temperature Trends and Variability in the Tropical Atmosphere

B. D. Santer,^{1*} T. M. L. Wigley,² C. Mears,³ F. J. Wentz,³
S. A. Klein,¹ D. J. Seidel,⁴ K. E. Taylor,¹ P. W. Thorne,⁵
M. F. Wehner,⁶ P. J. Gleckler,¹ J. S. Boyle,¹ W. D. Collins,²
K. W. Dixon,⁷ C. Doutriaux,¹ M. Free,⁴ Q. Fu,⁸ J. E. Hansen,⁹
G. S. Jones,⁵ R. Ruedy,⁹ T. R. Karl,¹⁰ J. R. Lanzante,⁷ G. A. Meehl,²
V. Ramaswamy,⁷ G. Russell,⁹ G. A. Schmidt⁹

The month-to-month variability of tropical temperatures is larger in the troposphere than at Earth's surface. This amplification behavior is similar in a range of observations and climate model simulations and is consistent with basic theory. On multidecadal time scales, tropospheric amplification of surface warming is a robust feature of model simulations, but it occurs in only one observational data set. Other observations show weak, or even negative, amplification. These results suggest either that different physical mechanisms control amplification processes on monthly and decadal time scales, and models fail to capture such behavior; or (more plausibly) that residual errors in several observational data sets used here affect their representation of long-term trends.

Tropospheric warming is a robust feature of climate model simulations that include historical increases in greenhouse gases (1–3). Maximum warming is predicted to occur in the middle and upper tropical troposphere. Atmospheric temperature measurements from radiosondes also show warming of the tropical troposphere since the early 1960s (4–7), con-

sistent with model results (8). The observed tropical warming is partly due to a step-like change in the late 1970s (5, 6).

Considerable attention has focused on the shorter record of satellite-based atmospheric temperature measurements (1979 to present). In both models and observations, the tropical surface warms over this period. Simulated surface warming is amplified in the tropical troposphere, corresponding to a decrease in lapse rate (2, 3, 9). In contrast, a number of radiosonde and satellite data sets suggest that the tropical troposphere has warmed less than the surface, or even cooled, which would correspond to an increase in lapse rate (4–12).

This discrepancy may be an artifact of residual inhomogeneities in the observations (13–19). Creating homogeneous climate records requires the identification and removal of non-climatic influences from data that were primarily collected for weather forecasting purposes. Different analysts have followed very different data-adjustment pathways (4–7, 12, 14, 17). The resulting “structural uncertainties” in ob-

served estimates of tropospheric temperature change (20) are as large as the model-predicted climate-change signal that should have occurred in response to combined human and natural forcings (16).

Alternately, there may be a real disparity between modeled and observed lapse-rate changes over the satellite era (9–11, 21). This disparity would point toward the existence of fundamental deficiencies in current climate models (and/or in the forcings used in model experiments), thus diminishing our confidence in model predictions of climate change.

This scientific puzzle provides considerable motivation for revisiting comparisons of simulated and observed tropical lapse-rate changes (10, 13, 21, 22) with more comprehensive estimates of observational uncertainty and a wide range of recently completed model simulations. The latter were performed in support of the Fourth Assessment Report of the Intergovernmental Panel on Climate Change (IPCC), and involve 19 coupled atmosphere-ocean models developed in nine different countries. Unlike previous model intercomparison exercises involving idealized climate-change experiments (23), these new simulations incorporate estimated historical changes in a variety of natural and anthropogenic forcings (24, 25).

Our focus is on the amplification of surface temperature variability and trends in the free troposphere. We study this amplification behavior in several different ways. The first is to compare atmospheric profiles of “scaling ratios” in the IPCC simulations and in two new radiosonde data sets: HadAT2 (Hadley Centre Atmospheric Temperatures, version 2) and RATPAC (Radiosonde Atmospheric Temperature Products for Assessing Climate). These were compiled (respectively) by the UK Met Office (UKMO) (6) and the National Oceanic and Atmospheric Administration (NOAA) (7). The scaling factor is simply the ratio between the temperature variability (or trend) at discrete atmospheric pressure levels and the same quantity at the surface (26). Observed trends and variability in tropical surface temperatures (T_s) were obtained from the NOAA (27) and HadCRUT2v data sets (28, 29).

¹Program for Climate Model Diagnosis and Intercomparison, Lawrence Livermore National Laboratory, Livermore, CA 94550, USA. ²National Center for Atmospheric Research, Boulder, CO 80303, USA. ³Remote Sensing Systems, Santa Rosa, CA 95401, USA. ⁴National Oceanic and Atmospheric Administration (NOAA)/Air Resources Laboratory, Silver Spring, MD 20910, USA. ⁵Hadley Centre for Climate Prediction and Research, UK Met Office, Exeter, EX1 3PB, UK. ⁶Lawrence Berkeley National Laboratory, Berkeley, CA 94720, USA. ⁷NOAA/Geophysical Fluid Dynamics Laboratory, Princeton, NJ 08542, USA. ⁸Department of Atmospheric Sciences, University of Washington, Seattle, WA 98195, USA. ⁹NASA/Goddard Institute for Space Studies, New York, NY 10025, USA. ¹⁰NOAA/National Climatic Data Center, Asheville, NC 28801, USA.

*To whom correspondence should be addressed. E-mail: santer1@llnl.gov

Supporting on line material

Supporting Text

The MSU instruments are cross-track scanning radiometers, which measure upwelling microwave radiation from the earth at a number of view angles spaced by 9.47° ($-47.35^\circ, -37.88^\circ, 28.41^\circ, \dots, 0.0, \dots, 47.35^\circ$), and at several different microwave frequencies on the lower shoulder of a complex of oxygen absorption lines near 57GHz. These view angles correspond to a range of Earth incidence angles from -56.2° to 56.2° , after taking into account the height of the satellite above the curved surface of the earth. The “MSU2” dataset is an average of MSU channel 2 data over the 5 near-nadir views, which measures radiation from a thick layer of the atmosphere from the surface to the lower stratosphere. Because of the longer path of the radiation for the views with larger incidence angles, the effective weighting function for these views peaks higher in the atmosphere than for the near nadir views. By calculating the weighted difference between the near limb views and views closer to nadir, an effective brightness temperature (Temperature Lower Troposphere, or TLT) can be retrieved with an effective weighting function that peaks several kilometers lower in the troposphere than MSU2 with much reduced stratospheric influence (*SI*). The reduction on stratospheric influence is coupled with a modest increase in the contribution of surface emission. The weights used to construct the datasets are made explicit in the equations below.

$$\begin{aligned}MSU2 &= 0.2(T_4 + T_5 + T_6 + T_7 + T_8) \\ TLT &= \frac{TLT_{left} + TLT_{right}}{2} \\ TLT_{left} &= 2(T_3 + T_4) - 1.5(T_1 + T_2) \\ TLT_{right} &= 2(T_8 + T_9) - 1.5(T_{10} + T_{11})\end{aligned}\tag{S1}$$

where T_i is the MSU channel 2 brightness temperature from the i^{th} view angle. View number 6 is the nadir view, and views 1 and 11 are the near limb views with incidence angle of approximately 56.2° . In Fig. S1, we show the vertical weighting functions for MSU2 and TLT separately for land and ocean scenes. The weighting functions over the ocean are modified due to the reduced emissivity of the ocean surface relative to land. Note that because of the differencing procedure used to compute TLT, errors or noise present in the measured brightness temperatures are amplified by a factor of about 5 relative to MSU2. This extra noise makes it more difficult to diagnose details of the TLT merging procedure, as much of the temporally coherent behavior we have used to investigate our MSU2 merging procedure is hidden in the noise for TLT.

As mentioned in the main text, we find that the Christy et al method used to estimate the diurnal correction is very sensitive to satellite attitude. Christy et al. estimate the diurnal signal by taking the difference between TLT_{left} and TLT_{right} , and using that difference to estimate the rate of change of TLT as a function of local time, which differs for the left and right side of the swaths. Using long-term mean atmospheric profiles from the NCEP reanalysis (S2) as input for a radiative transfer model (S3), we calculated the

sensitivity of the $TLT_{\text{left}} - TLT_{\text{right}}$ to a change in satellite roll angle. Zonally averaged values for the sensitivity range from 1.7 K/degree in the tropics to 0.8 K/degree near the poles, reflecting the decrease in average lapse rate as one moves away from the equator. A typical value of the rate of change of the global average of TLT due to the diurnal cycle, when the ascending and descending nodes are combined, is about 0.025 K/hour. This magnitude is consistent with both our climate-model-based estimate and from the Christy et al. estimate from cross scan differences, though these estimates differ in sign. This rate of change yields a cross-scan difference (for a cross-scan time difference of 0.71 hours, the value at the equator) of about 0.018K, corresponding to a roll error of 0.01° . Near the poles, the corresponding roll angle is several times larger, due to both the reduced sensitivity to roll angle, and to the increased cross-scan time difference. However, the 0.01° value is valid throughout the tropics, where the largest discrepancy between this work and the Christy et al. results occurs. The satellite attitude would need to be known even more accurately than 0.01° to determine the details of the diurnal correction well enough to perform a credible adjustment for the effects of changes in LECT. The pointing accuracy requirements for these NOAA satellites is 0.12° , more than 10 times larger than the required accuracy (S4). Researchers using infra-red and visible imagery from these satellites typically need to make cross-track earth location adjustments of about 1 km to ensure accurate registration with known earth targets (S5). An Earth location error of 1.0 km corresponds to pointing error of about 0.07 degrees for the NOAA satellites.

In an attempt to mitigate this problem, Christy et al. used a combination of ascending and descending measurements that removed the effect of any constant error in satellite attitude. However, any systematic “wobble” in the satellite roll of the order of 0.01° will cause error in the derived diurnal correction. The MSU spacecraft use an Earth Sensor Assembly (ESA) to determine the spacecraft roll and pitch by making infrared measurements of the horizon. The ESA was designed for a 0.12° (2σ) accuracy in determining roll and pitch (S4), an order of magnitude less accurate than that required by the Christy et al. method. The operational characteristics of the ERA probably vary slightly for day viewing versus night viewing, and a systematic 0.01° variation would not be unreasonable. Furthermore, analyses of infrared and visible imagery from the MSU spacecraft obtained from the AVHRR sensor indicates the true pointing accuracy only barely meets the 0.12° requirement (S5).

We have calculated model derived diurnal cycles for both MSU2 and TLT. We show the results of the T2 calculations here to highlight some important regional differences between our diurnal correction and the Christy et al correction. In Fig S2A and S2B, we show a color-coded time-latitude plot of the diurnal correction applied to MSU2 by each group for the NOAA-11 satellite (S6) to account for its drift in LECT during the time period shown. Since this correction is applied to the combined data from ascending and descending parts of the orbit, the correction reflects the combined effects of early morning and mid-afternoon temperature changes. The Mears et al. MSU2 model-based diurnal correction (Fig S2B) is much smoother as a function of latitude, and shows the correction in ocean-dominated latitudes is small, in accordance with expectations. In contrast, the UAH MSU2 correction (Fig. S2A) has two features that lead us to doubt its accuracy on the regional scale. First, adjacent latitudes often have radically different corrections, most notably in the region from 42S to 30S. Second, a large correction is

applied to the region between 60S and 45S, where the Earth is almost entirely ocean. Oceanic regions have much reduced diurnal cycles relative to land areas due to reduced surface warming.

The major drawback of our method is that it is based on output from a climate model (CCM3). A subsequent version of the climate model, the Community Climate System Model, has been shown to have significant problems with its representation of the diurnal cycle in the troposphere, though the largest problems were with precipitation, not temperature (S7). Also, the ocean surface that forms the lower boundary layer in the CCM3 model has no diurnal variability. Even though this diurnal variability is small in most locations and weather conditions (S8), it could lead to important errors in the diurnal cycle due to the large area of the oceans. To help increase our confidence in the model-derived diurnal cycle, we examine the MSU data in ways that provide important information about the spatial (both location and vertical) and seasonal structure of the diurnal cycle. In addition to helping to validate the model-based diurnal cycle, the findings can be used to add weight to our arguments about similarity of the time dependence of the MSU2 and TLT diurnal cycles.

In Figure S3, we plot, as an example, the difference in brightness temperature between the ascending and descending measurements made by NOAA-11 during the summer of 1990. The mean LECT of the NOAA-11 satellite for this time period was 2:07 PM, near the afternoon peak of the diurnal cycle, so the difference between the ascending and descending measurements, separated by approximately 12 hours, provides information about the relative amplitude of the first harmonic of the diurnal cycle for different earth locations and fields of view. For all three zonal bands, the amplitude of the diurnal cycle over the ocean is only a small fraction of that over land. Over land, the amplitude is strongly attenuated for the near limb views (view numbers 1,2,10,11) relative to the near-nadir views (view numbers 5,6,7), suggesting that the bulk of the diurnal cycle comes from at or near the surface. In fact, fits made by assuming the surface is the only source of diurnal cycle fit the data very well in the tropical and northern bands (panels b and e). Problems with the fit in the Southern band are probably related to sampling error due to the limited amount of land data available in this band. When the land and ocean data are combined in the third column, multiplied by the appropriate land/ocean area weighting factors, the land signature dominates.

The open squares are the ascending-descending differences plotted after our diurnal adjustment has been applied. These plots show that our model-based diurnal correction does a good job of explaining the majority of the ascending-descending differences, especially in the tropical and northern bands, thus validating the first harmonic of our diurnal cycle. The fact that the model removes the ascending-descending differences from all views simultaneously indicates that the vertical structure of the diurnal cycle is well captured by the model. The southern band appears to have a small additional offset that is independent of view angle, which is probably due to spurious calibration effects that we have not yet diagnosed.

Before merging data from the different satellites together, each MSU instrument needs to be separately calibrated so that it agrees with other instruments in the MSU series. This is performed by comparing measurements of the earth during periods of overlapping operation between satellite pairs. Christy et al. have developed an empirical formula that

accurately describes the time dependence of spatially averaged intersatellite differences (S9, S10)

$$T_{Meas,i} = T_0 + A_i + \alpha_i T_{Target,i} + \varepsilon_i \quad (S2)$$

Here $T_{Meas,i}$ is the brightness temperature measured by the i^{th} satellite, T_0 is the actual brightness temperature of the earth, A_i is a constant offset for each satellite, and α_i is a small “target factor” that describes the correlation of the measured temperature with the temperature of the hot calibration target on the i^{th} satellite, $T_{Target,i}$, and ε_i represents residual differences due to instrument noise and differences in spatial-temporal sampling between co-orbiting instruments.

We perform the construction of a multi-satellite, monthly, gridded MSU TLT data product as follows. First, we apply the diurnal adjustment to each measurement so that the measured brightness temperature corresponds to local noon. Then, we estimate a set of target factors α_i . and offsets A_i . To determine these merge parameters from the MSU data, we calculate 5-day, global averages of brightness temperature. For each 5 day period where two (or more) satellites are making measurements simultaneously, we form an equation by differencing versions of Eq. S1 for the two satellites in question,

$$T_{Meas,i} - T_{Meas,j} = A_i - A_j + \alpha_i T_{Target,i} - \alpha_j T_{Target,j} + \varepsilon_i - \varepsilon_j. \quad (S3)$$

Over the period of operation for the MSU series of satellites, this procedure yields about 1100 equations in 17 unknowns (S11). The solution to the equation is then found using singular value decomposition, thus determining the values of the merging coefficients. It is important to note that because the diurnal correction is applied before this regression procedure, errors in the diurnal correction (or omission of it entirely) can influence the values of the merging coefficients. To reduce the effects of any errors in the diurnal cycle on the retrieved merging parameters, we choose to determine the target factors for our final dataset using ocean-only data from MSU2, which has a small diurnal cycle, and minimal “noise” associated with the interaction of spatial sampling with day-to-day variability in surface heating. We view this to be the most accurate way to determine the target factors. We consider these parameters to be constants that describe the behavior of the radiometer, and thus can be applied to other linear combinations of MSU channel 2 views, including TLT. Note that the use of TLT data directly in a similar regression procedure could possibly lead to values that are less well determined due to noise amplification caused by the differencing procedure used to create TLT. However, in the interest of completeness, and to help quantify uncertainty, we also report the consequences of other choices of target factors on global trends in TLT later in this discussion.

After determining the merging coefficients, we apply Eq. S1 to calculate T_0 , the homogenized brightness temperature, for each measurement. These are then used to calculate TLT, separately for the left and right sides of the measurement swath. These are then averaged into in daily, 2.5° by 2.5° bins, assuming that the TLT average represents the tropospheric temperature for all the footprints that were used in its calculation. The daily time series at each grid point are then assembled into monthly averages taking care

to exclude obvious outliers, and a gridded monthly anomaly dataset is calculated by removing the average seasonal cycle over the 20 year period from 1979-1998. Linear trends can be calculated at each point to make trend maps such as those shown in Fig. 3.

For the MSU2 case, we find the differences in values for the target multipliers of two of the nine satellites, NOAA-09 and NOAA-11 account for about 75% of the difference in global trends between our work(S10) and that of Christy et al. (S12). The results of an experiment where we fix values of the target factors to the Christy et al. values is summarized in table S1 below. The origin of these difference in target factors is the different choices made by our two groups for the data used as input to the regression procedure. We use all available data from overlapping satellites, while Christy et al. restrict their attention to satellite overlaps with durations longer than 2 years when determining their target factors (S10, 12). Note that the conclusion that the differences between our MSU2 datasets is mostly determined by differences in the NOAA-09 and NOAA-11 target factors only applies to global time series. For time series constructed for regions with less than global extent, the regional differences between our diurnal corrections will become important, and lead to substantial additional differences between regional time series.

In contrast, for the TLT case, the difference between chosen target factors accounts for a smaller part of the difference between our results, particularly in the tropics. We conducted a numerical experiment where we determined the target factors using a number of different data subsets as input to the regression procedure discussed above. For completeness, we also include the Christy et al target factors. These target factors were then used to merge the data from the 9 satellites, and global and tropical trends were calculated, with the intersatellite offsets recalculated for each case. In Fig. S3, we plot the values for the target factors, and the trend results are summarized in Table S2. In the global case, the choice of target factors accounts for slightly less than 50% of the difference in reported trends, while in the tropics, it accounts for less than 25% of the difference. When TLT data are used as input to the regression procedure, the target factors obtained tend to result in slightly smaller decadal trends, though when the same set of near-limb views is used, but without the weighting differencing used to calculate TLT (which, as noted above, amplifies noise), target factors are obtained that result in larger decadal trends. We used the spread in these trends to help evaluate the uncertainty in our reported trends.

Note that the merging method we use here is fundamentally different than that used by Grody et al. (S13). They introduced a physically based model of MSU error to replace the empirical models used by Christy et al. and Mears et al.. The Grody et al. error model explicitly included radiometer non-linearity and temperature errors in both the hot and cold loads. We have used their error model in our merging methodology with less than a 5% change in long-term global trends, suggesting that the differences between our MSU results and the Grody et al. results are caused not by any difference in error model, but rather by differences in the merging procedure. Two procedural differences that we are aware of that might cause important differences are noted here. (1) Grody et al. perform a long-term temporal average before solving for the merging parameters. (2) Grody et al do not perform any diurnal correction before deducing the parameters of their model. A previous version of this dataset (S14) did not include any correction for radiometer non-linearity or hot or cold load errors.

In the following paragraphs we estimate the uncertainty range for decadal trends in TLT. We consider three types of uncertainty, which we call internal uncertainty, structural uncertainty, and statistical uncertainty.

Internal uncertainty is the uncertainty that arises once a method is chosen, due to a finite sample of noisy data. In our case, this is the uncertainty that arises from the regression procedure after the diurnal correction and a method of determining the target factors has been chosen. Calculation of this type of uncertainty is straightforward within the framework of our regression based procedure for determining the merging coefficients. Using methods identical to the Monte Carlo methods we use to assess this type of uncertainty for MSU2 (*S10*), we find the 1- σ internal uncertainty for the TLT merge to be 0.019K/decade. As is the case for MSU2, most of this uncertainty is associated with uncertainty in determining the values of the target factor for the NOAA-09, due to its short period of overlap with other satellites.

Structural uncertainty results when the results depend on choices made concerning the methods used in constructing the dataset. As defined in the context of dataset constructed for the study of climate change, the range of choices would contain all “physically reasonable” methods of dataset construction (*S15*). Here we restrict our analysis to the different sets of target factors discussed above, and to the effects of a possible overall multiplicative error in our diurnal adjustment. From Table S2, the 1- σ spread in trends due to different methods of determining target factors is 0.033K/decade. Figure S2 (and other, similar analysis for other satellites and other three month periods) suggests that the first harmonic our diurnal cycle is accurate to about 10%. Allowing for the possibility that the model is less accurate for the higher harmonics which dominate the diurnal corrections, we performed an experiment where we varied the applied diurnal correction by +/- 25%. This results in a change in TLT global trend of +/-0.024. Combining these estimates in an RMS fashion results in an estimate of structural uncertainty of 0.041K/decade. When the internal uncertainty is also included, we obtain an uncertainty estimate of 0.045K/decade (1- σ , or 0.09 K/decade, 2- σ) for these two types of uncertainty combined.

Statistical uncertainty is a measure of how well the given time series fits the underlying assumed model, in this case, a linear trend. Whether or not it is appropriate to include this uncertainty in the total uncertainty in the trend estimate depends on the question under consideration. Time series of MSU tropospheric data are dominated by large interannual fluctuations, caused, for example, by ENSO events. These fluctuations result in large statistical uncertainty estimates, on the order of 0.2K/decade (*S16*). When datasets that are different measurements of the same variable (e.g. two different realization of satellite-derived TLT) are examined, we find that the interannual fluctuations are very similar (*S16*). When comparing trends calculated for two such similar datasets, the focus of this report, it is not appropriate to include this statistical uncertainty when deciding if they agree within uncertainty limits. Note that the statistical uncertainty in the fitted trends is an appropriate measure for doing other kinds of comparisons, for example when comparing MSU data to fully coupled climate model output. These models also typically large interannual fluctuations due to ENSO events, but these fluctuations tend to occur at different times in the time series since the times that ENSO events occur are not constrained to match the actual events (*S17, 18*).

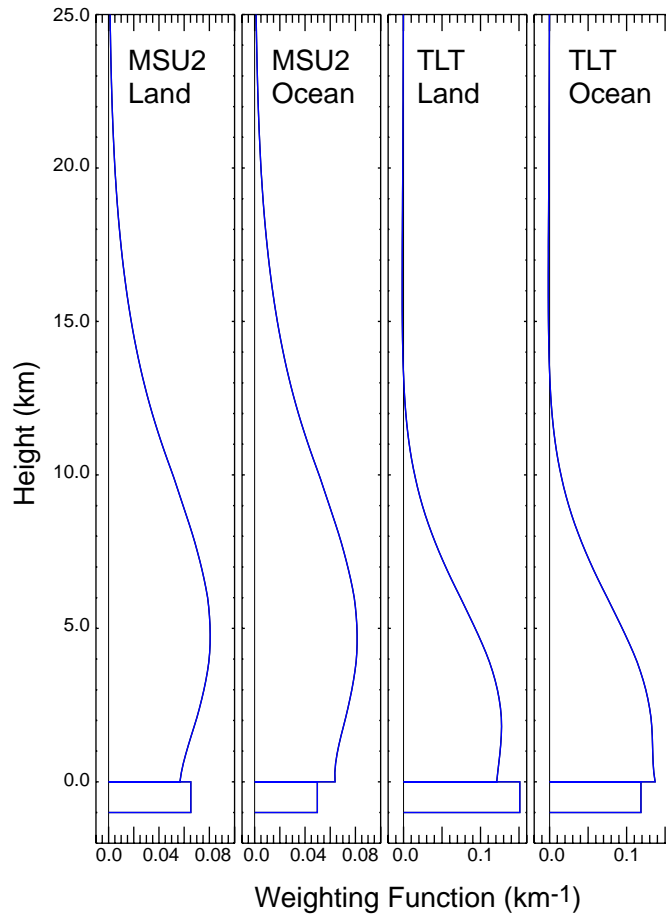


Fig. S1. Vertical weighting functions for MSU2 and TLT, for land and ocean scenes. The part of the weighting function due to surface emission is represented by the rectangle at the bottom of the figure. These weighting functions are computed using the US standard atmosphere, with a surface relative humidity of 70%, and a water vapor scale height of 1.5 km. We also assume that the land surface is at sea level. For actual land views, the surface weight is often considerably larger because the elevation of the surface is above sea level.

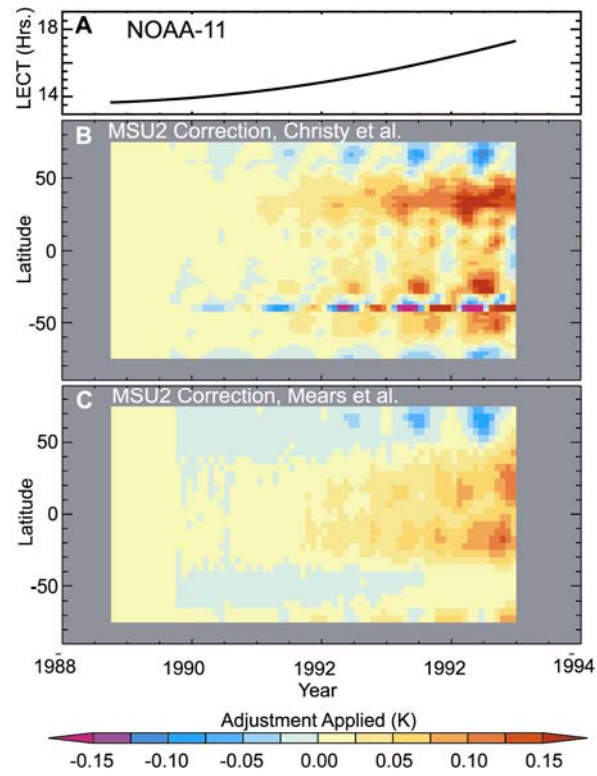


Fig. S2. Diurnal correction applied to MSU2 for the NOAA-11 satellite. (A) LECT for the NOAA-11 satellite. (B) MSU2 correction applied by Christy et al. (c) MSU correction applied in this work.

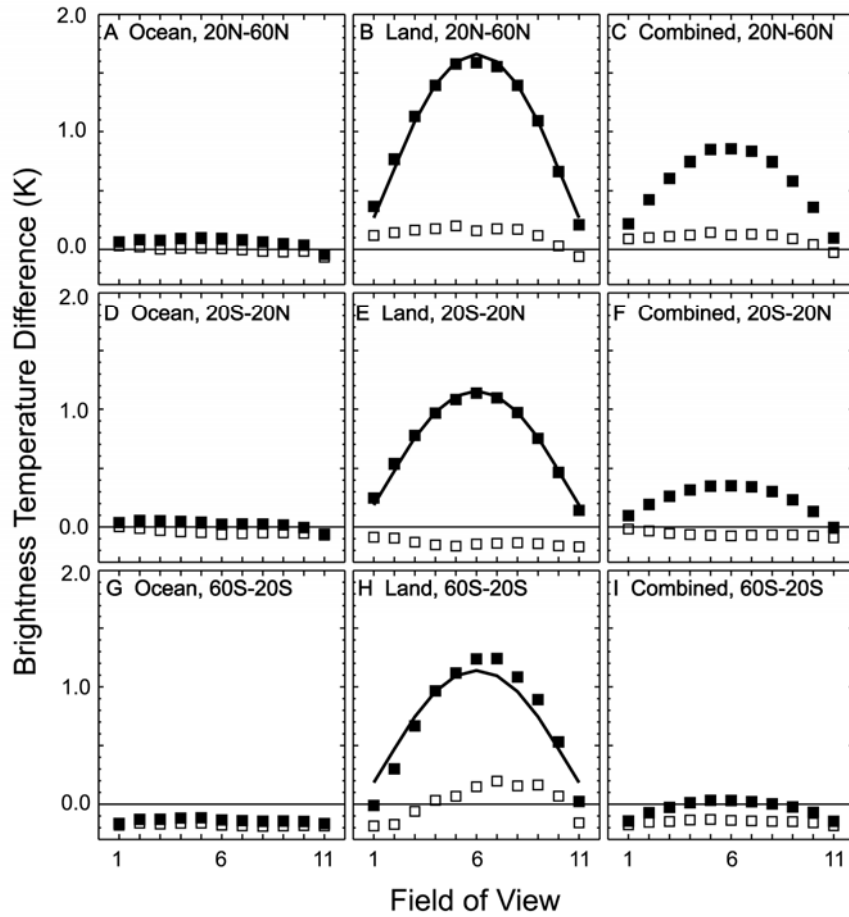


Fig. S3. Mean difference of brightness temperatures measured on the ascending and descending parts of the orbit (solid squares), plotted for three zonal bands, and for ocean, land and combined land and ocean data subsets. The data presented here are from NOAA-11, averaged over June, July, and August of 1990. The open squares are mean ascending-descending differences after our diurnal adjustment has been applied to the data, and the solid curves on the land plots are a simple fit to the FOV dependence made by assuming all of the signal arises from the surface.

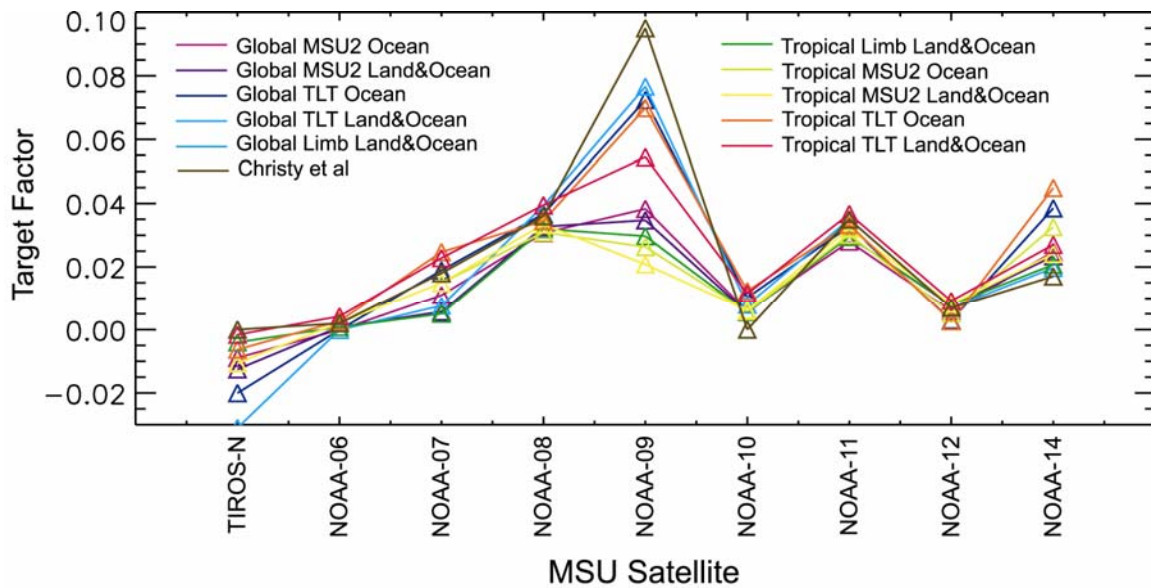


Fig. S4. Different values for the target factors determined by using different types of data as input to the regression procedure used to calculate the target factors and intersatellite offsets. The largest changes occur for the target factor for NOAA-09, which is poorly determined due to its short overlap times with other satellites. Examination of the covariance matrix from the regression procedure also indicates that it is poorly determined. Datasets that use TLT data tend to produce larger target multipliers for NOAA-09 and smaller trend values (see Table S2). As noted in the main text, we choose not to use these sets to produce our definitive dataset because the increased noise in the TLT data can lead to erroneous determination of the target multipliers. Instead, we use the target factors found using MSU2 (purple curve). The UAH target factors (brown curve) show an even larger value for the NOAA-09 target factor.

Table S1. Results of an experiment where MSU2 target factors for the NOAA-09 and NOAA-11 satellites are set to the values used by Christy et al. The other target factors were recalculated in each case to minimize global intersatellite differences. The results indicate the most of the difference in the long-term global MSU2 trends for our two datasets is due to differences in these two merge parameters.

NOAA-09 Target Factor	NOAA-11 Target Factor	Trends in MSU2, 1979-2004 (K/decade)	percent of difference from Christy et al. explained
Mears et al.	Mears et al.	0.128	--
Mears et al.	Christy et al.	0.110	23%
Christy et al.	Mears et al.	0.089	49%
Christy et al.	Christy et al.	0.070	73%

Table S2. Global and Tropical (20S to 20N) Trends in TLT over the 1979-2003 period that result when we use different types of data as input to the regression procedure we use to determine the target multipliers. The use of TLT data in the regression tends to result in smaller trends, while the use of data from the limb views (views 1-4,7-11) averaged together (the same views as are used to calculate TLT, but without the weighted differencing procedure) results in target factors that produce larger trends when used to merge TLT data. The spread in trends here ($\sigma = 0.033$ global, 0.025 tropical) can be used to estimate part of the structural uncertainty in our reported trend number. We choose to use the MSU2 Ocean target factors when producing the final dataset reported here because these target factors are the least likely to be influenced by a incorrect diurnal correction or by noise. The last row shows the trends reported on Christy et al for reference.

Data used in regression to determine target factors	Global TLT Trend(K/dec.)	Tropical TLT Trend (K/dec.)
MSU2 Ocean	0.193	0.189
MSU2 Land and Ocean	0.200	0.203
TLT Ocean	0.137	0.153
TLT Land and Ocean	0.157	0.161
Limb Only	0.209	0.208
UAH target factors	0.144	0.145
Christy et al.	0.087	-0.015

Table S3. Global and Tropical (20S to 20N) Trends (C/decade) in TLT using different combinations of the diurnal correction and target factors. Results are shown for a shorter period (1979-2001) because the Christy et al diurnal correction is not available after October 2002. In each case, the offsets were recalculated to minimize intersatellite differences. When we apply both the diurnal correction and the target factors from Christy et al, we calculate trends that show even less warming (or more cooling) than results reported in Christy et al (shown on the bottom row), suggesting that there are other differences in methodology that are not captured by the diurnal correction and the target factors. These differences result in small trend differences that limit our ability to exactly state the portion of the trend difference caused by the difference in diurnal correction. The results do indicate that over 55% of the difference in global trends is caused by the difference in diurnal correction. In the tropics, where the difference in diurnal correction is largest, over 70% of the difference is due to the diurnal correction.

Diurnal Correction	Target Factors	Global Trend (K/dec)	Tropical Trend (K/dec)
Mears et al	Mears et al	0.169	0.160
Christy et al	Mears et al	0.085	-0.006
Mears et al	Christy et al	0.108	0.098
Christy et al	Christy et al	0.023	-0.068
Christy et al (2003) results		0.058	-0.044

Supporting References and Notes

- S1. R. W. Spencer, J. R. Christy, *J. Clim.* **5**, 858 (1992).
- S2. E. Kalnay *et al.*, *Bull. Amer. Meteor. Soc.* **77**, 437 (1996).
- S3. F. J. Wentz, T. Meissner, AMSR Ocean Algorithm Theoretical Basis Document *Tech. Report No. 121599A-1* (Remote Sensing Systems, 2000).
- S4. A. Schwalb. (1978), NOAA Technical Memorandum NESS 95, pp. 75.
- S5. G. Rosborough, D. Baldwin, W. J. Emery, *IEEE Trans. on Geoscience and Remote Sens.* **32**, 644 (1994).
- S6. We use NOAA-11 as an example because it underwent significant drift in LECT during its lifetime. We have plotted our diurnal adjustment to reflect the way the Christy et al apply their diurnal adjustment -- they adjust each monthly average so that it corresponds to the local measurement time for same month in the first year of each satellites observations. In contrast, we adjust each measurement to local noon. This introduces a stationary seasonal cycle into the diurnal adjustment that is not plotted here.
- S7. A. Dai, K. E. Trenberth, *J. Clim.* **17**, 930 (2004).
- S8. C. L. Gentemann, C. J. Donlon, A. Stuart-Menteth, F. J. Wentz, *Geophys. Res. Lett.* **30**, 1140 (2003).
- S9. J. R. Christy, R. W. Spencer, W. D. Braswell, *J. of Atmos. Ocean. Tech.* **17**, 1153 (2000).
- S10. C. A. Mears, M. C. Schabel, F. J. Wentz, *J. Clim.* **16**, 3650 (2003).
- S11. One offset A_i must be set to an arbitrary value to obtain a solution. We set the offset for the NOAA-10 satellite to zero. This choice only introduces a constant offset to the entire dataset, and thus has no effect on the anomaly time series and trends.
- S12. J. R. Christy, R. W. Spencer, W. B. Norris, W. D. Braswell, D. E. Parker, *J. of Atmos. Ocean. Tech.* **20**, 613–629 (2003).
- S13. N. C. Grody, K. Y. Vinnikov, M. D. Goldberg, J. T. Sullivan, J. D. Tarpley, *J. Geophys. Res.* **109** (2004).
- S14. K. Y. Vinnikov, N. C. Grody, *Science* **302**, 269 (2003).
- S15. P. W. Thorne, D. E. Parker, J. R. Christy, C. A. Mears, *Bull. Amer. Meteor. Soc.* (in press) (2005).
- S16. D. J. Seidel *et al.*, *J. Clim.* **17**, 2225 (2004).
- S17. B. D. Santer *et al.*, *Science* **300**, 1280 (2003).
- S18. B. D. Santer *et al.*, *Science* (submitted) (2005).